



HAL
open science

Splitting kinetics of Si_{0.8}Ge_{0.2} layers implanted with H or sequentially with He and H

P. Nguyen, K.K. Bourdelle, C. Aulnette, F. Lallement, N. Daix, N. Daval, I. Cayrefourcq, F. Letertre, C. Mazuré, Y. Bogumilowicz, et al.

► To cite this version:

P. Nguyen, K.K. Bourdelle, C. Aulnette, F. Lallement, N. Daix, et al.. Splitting kinetics of Si_{0.8}Ge_{0.2} layers implanted with H or sequentially with He and H . Journal of Applied Physics, 2008, 104, pp.113526. 10.1063/1.3033555 . hal-01736059

HAL Id: hal-01736059

<https://hal.science/hal-01736059v1>

Submitted on 23 Mar 2018

HAL is a multi-disciplinary open access archive for the deposit and dissemination of scientific research documents, whether they are published or not. The documents may come from teaching and research institutions in France or abroad, or from public or private research centers.

L'archive ouverte pluridisciplinaire **HAL**, est destinée au dépôt et à la diffusion de documents scientifiques de niveau recherche, publiés ou non, émanant des établissements d'enseignement et de recherche français ou étrangers, des laboratoires publics ou privés.

Splitting kinetics of $\text{Si}_{0.8}\text{Ge}_{0.2}$ layers implanted with H or sequentially with He and H

Phuong Nguyen, K. K. Bourdelle, C. Aulnette, F. Lallement, N. Daix, N. Daval, I. Cayrefourcq, F. Letertre, C. Mazuré, Y. Bogumilowicz, A. Tauzin, C. Deguet, N. Cherkashin, and A. Claverie

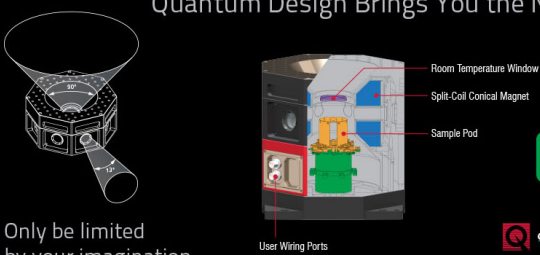
Citation: *Journal of Applied Physics* **104**, 113526 (2008); doi: 10.1063/1.3033555

View online: <https://doi.org/10.1063/1.3033555>

View Table of Contents: <http://aip.scitation.org/toc/jap/104/11>

Published by the [American Institute of Physics](#)

Quantum Design Brings You the Next Generation Magneto-Optic Cryostat




Only be limited by your imagination...

[Learn More](#)

Quantum Design
qdusa.com/opticool5

8 Optical Access Ports: 7 Side; 1 Top
Temperature Range: 1.7 K to 350 K
7 T Split-Coil Conical Magnet
Low Vibration: <10 nm peak-to-peak
89 mm x 84 mm Sample Volume
Automated Temperature & Magnet Control
Cryogen Free



Splitting kinetics of $\text{Si}_{0.8}\text{Ge}_{0.2}$ layers implanted with H or sequentially with He and H

Phuong Nguyen,^{1,a)} K. K. Bourdelle,¹ C. Aulnette,¹ F. Lallement,¹ N. Daix,¹ N. Daval,¹ I. Cayrefourcq,¹ F. Letertre,¹ C. Mazuré,¹ Y. Bogumilowicz,² A. Tauzin,² C. Deguet,² N. Cherkashin,³ and A. Claverie³

¹SOITEC, Parc Technologique des Fontaines, Bernin 38926, Crolles Cedex, France

²CEA-LETI-Minatec, 17 Rue des Martyrs, 38054 Grenoble Cedex 9, France

³CEMES/CNRS, nMat Group, BP 4347, F-31055 Toulouse, France

(Received 25 July 2008; accepted 16 October 2008; published online 9 December 2008)

We have performed systematic measurements of the splitting kinetics induced by H-only and He +H sequential ion implantation into relaxed $\text{Si}_{0.8}\text{Ge}_{0.2}$ layers and compared them with the data obtained in Si. For H-only implants, Si splits faster than $\text{Si}_{0.8}\text{Ge}_{0.2}$. Sequential ion implantation leads to faster splitting kinetics than H-only in both materials and is faster in $\text{Si}_{0.8}\text{Ge}_{0.2}$ than in Si. We have performed secondary ion mass spectrometry, Rutherford backscattering spectroscopy in channeling mode, and transmission electron microscopy analyses to elucidate the physical mechanisms involved in these splitting phenomena. The data are discussed in the framework of a simple phenomenological model in which vacancies play an important role. © 2008 American Institute of Physics. [DOI: 10.1063/1.3033555]

I. INTRODUCTION

Strained Si (*s*-Si) layers are attractive for advanced complementary metal-oxide semiconductor technologies because of the large enhancements of carrier mobilities they offer.¹ The fabrication of *s*-Si on insulator (*s*-SOI) structures adds to the traditional SOI technology the advantage of providing “substrates” with better performances in terms of mobility, transconductance, and drive current. These benefits have been recently demonstrated through the fabrication of partially and fully depleted planar transistors, as well as of three dimensional FinFET-fin field effect transistors.^{2–4} The fabrication of *s*-SOI wafers using the Smart Cut™ technology has been demonstrated.^{5–8} To fabricate such wafers, a layer detachment must occur in the SiGe film, which has served as a template for growing *s*-Si by epitaxy. We reported the studies of splitting kinetics involved H implantation into SiGe layers with different Ge concentrations.⁹ We also showed that, by using He and H sequential implantation instead of H-only implantation, the total implantation dose needed to achieve full splitting of the $\text{Si}_{0.8}\text{Ge}_{0.2}$ layers can be divided by a factor of 3.⁹

In this article we study in detail the splitting kinetics of $\text{Si}_{0.8}\text{Ge}_{0.2}$ substrates implanted with H-only or sequentially implanted with He and then with H. These data are compared with the kinetics obtained for bulk Si substrates. The extensive physical characterization of the implanted and annealed substrates provides important insights into the mechanism of splitting in $\text{Si}_{0.8}\text{Ge}_{0.2}$.

II. EXPERIMENTS

Relaxed SiGe layers of 1–2 μm thickness with uniform Ge content of 20% were grown on 200 mm (001) Si sub-

strates by the reduced pressure-chemical vapor deposition technique using a well known graded buffer approach.⁵ X-ray diffraction analysis confirmed the good crystalline quality and a relaxation degree of about 95%–98% of the layers. Dislocation densities measured by wet chemical revelation are typically in the 10^4 cm^{-2} range. 20-nm-thick *s*-Si layers were subsequently grown on the $\text{Si}_{0.8}\text{Ge}_{0.2}$ templates. The phonon wave number of this *s*-Si layer, given by Raman spectroscopy, is found at $514 \pm 0.2 \text{ cm}^{-1}$, which is in very good agreement with the expected value determined with a 20% Ge fraction and no strain in the SiGe virtual templates. In the following, the *s*-Si/ $\text{Si}_{0.8}\text{Ge}_{0.2}$ /Si structures will be simply named “SiGe” or “ $\text{Si}_{0.8}\text{Ge}_{0.2}$ ” samples since the fracture phenomenon occurs within the $\text{Si}_{0.8}\text{Ge}_{0.2}$ layer.

H-only implantations in the SiGe samples and reference (001) Si substrates through a 145-nm-thick oxide were carried out at doses and energies in the $(5–10) \times 10^{16} \text{ cm}^{-2}$ and (20–50 keV) ranges, respectively. For the sequential implantations, He was implanted first with energies for which the resulting depth profiles were somewhat deeper than the H profiles, but still close to the surface, in the region far from the graded buffer layer. Total doses (He+H) in the range of about $(2–3) \times 10^{16} \text{ cm}^{-2}$ were used. Direct bonding of the SiGe and Si implanted wafers with Si substrates was then performed. The bonded pairs were isothermally annealed at different temperatures until fracture occurred.

Some $\text{Si}_{0.8}\text{Ge}_{0.2}$ and Si samples have been annealed at moderate temperature (300–400 °C) for a few minutes. The He and H depth profiles were obtained by secondary ion mass spectrometry (SIMS). Rutherford backscattering spectroscopy (RBS) was used to measure the damage/defect distributions in the as-implanted and annealed samples. Cross sectional TEM (XTEM) was used to study the microstructure of the layers. Statistical analysis of the populations of H

^{a)}Electronic mail: phuong.nguyen@soitec.fr.

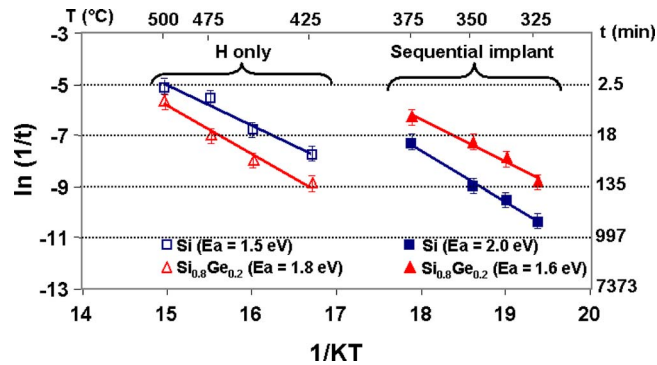


FIG. 1. (Color online) Splitting kinetic curves for Si and $\text{Si}_{0.8}\text{Ge}_{0.2}$ with H-only and He+H sequential implants.

(He)-related defects was performed on images taken under specific imaging conditions to access to their size and depth distributions.¹⁰

III. RESULTS

Figure 1 summarizes the results we obtained when measuring the time needed for the splitting of the layers during annealing at various temperatures for H-only and He+H sequentially implanted Si and SiGe samples. In agreement with our previous report⁹ for H-only implants, splitting is significantly slower in SiGe than in Si. Moreover, the sequential He+H implantations result in a faster splitting than the H-only implantations, both in Si and SiGe layers. Alternatively, the same splitting times can be obtained by annealing at much lower temperatures. This benefit is even larger in the case of SiGe layers. In other words, splitting occurs faster in Si than in SiGe when H-only is implanted, while it occurs slower in Si than in SiGe when He and H are sequentially implanted.

The Arrhenius-type plot presented in Fig. 1 allows us to extract an apparent “activation energy for splitting” from the

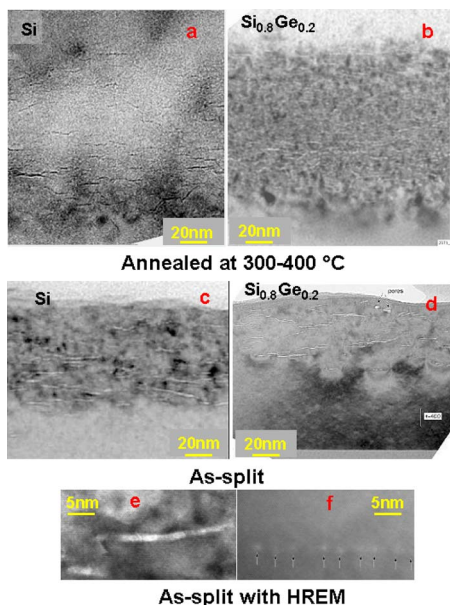


FIG. 2. (Color online) XTEM micrographs of annealed at moderate temperature and as-split Si and $\text{Si}_{0.8}\text{Ge}_{0.2}$ samples implanted with H-only.

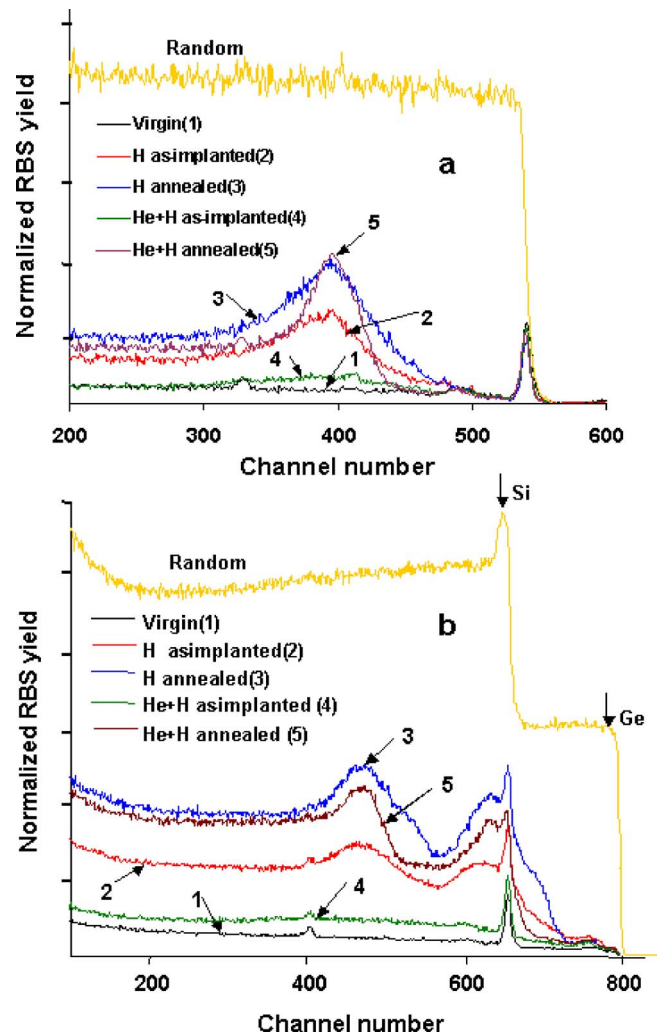


FIG. 3. (Color online) RBS channeling spectra for H-only and sequentially implanted Si and $\text{Si}_{0.8}\text{Ge}_{0.2}$ samples in the as-implanted state and after annealing at moderate temperature. A random spectrum is shown for reference.

results. For H-only implanted samples, this activation energy is smaller (1.5 eV) in Si than in SiGe (1.8 eV), while it is larger in Si (2 eV) after sequential implantation than in SiGe (1.6 eV). These numbers confirm that it is easier to split Si than SiGe layers with the single H implants, while it is more difficult to split Si than SiGe layers with the sequential implantation.

Figure 2 shows a set of typical XTEM images of the H-only implanted Si and $\text{Si}_{0.8}\text{Ge}_{0.2}$ samples after annealing at moderate temperature in the 300–400 °C range and after layer transfer obtained in the 500–550 °C range. After annealing at moderate temperature [Figs. 2(a) and 2(b)], (001) H-filled platelets of average sizes ranging from 15 to 20 nm are depth distributed over about 210 nm. There are no significant differences between the populations of platelets found in the Si and SiGe samples except that, owing to the higher stopping power of the H ions in SiGe, the platelets are located at a somewhat smaller distance from the surface. However, after splitting [Figs. 2(c) and 2(d)], the samples are clearly different. Large platelets and/or microcracks are seen in both layers, but being clearly larger in Si than in SiGe. Moreover, high resolution electron microscopy images, taken

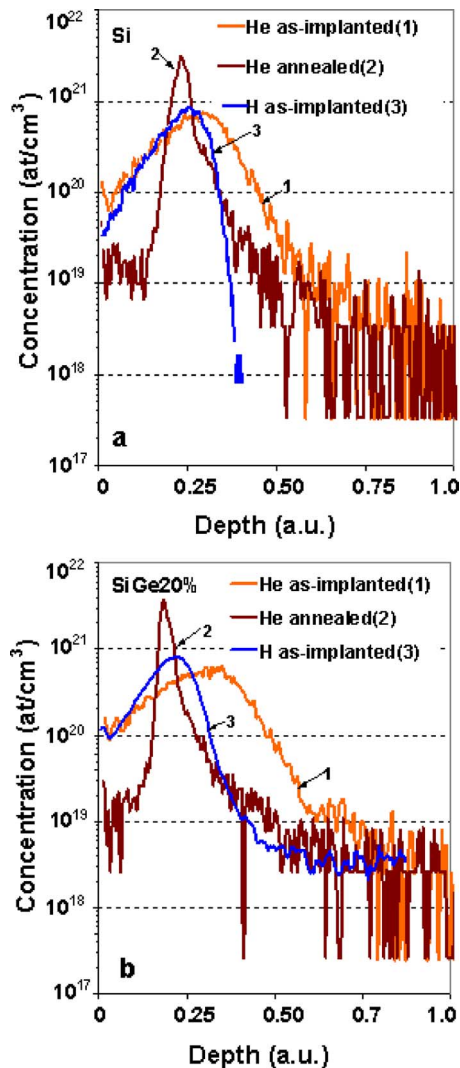


FIG. 4. (Color online) SIMS profiles of H and He in as-implanted and annealed Si and $\text{Si}_{0.8}\text{Ge}_{0.2}$ samples. A 1450-Å-thick oxide was removed before analysis of the samples.

near the surface, show that in SiGe [Fig. 2(f)] [and not in Si, Fig. 2(e)], these platelets have partially broken up into small pores that are aligned on a (100) plane. Isolated nanovoids could also be evidenced in some places.

Figure 3 shows the aligned ($\langle 001 \rangle$ axis) and random RBS spectra obtained for H-only and sequentially implanted Si and SiGe samples in the as-implanted state and after annealing at moderate temperature for a few minutes. In Si, it is clearly seen that while the damage level found in the as-implanted state is smaller after sequential implantation than after H-only implantation, after annealing, the situation is opposite, i.e., the damage profile in the sample sequentially implanted with He and H is slightly higher and considerably sharper [Fig. 3(a)].

The SiGe spectra [Fig. 3(b)] are more complicated to interpret since they are composed of backscattering contributions from the SiGe and from the *s*-Si top layers, which overlap around channels 620–650. For simplicity and for comparison with the case of Si substrates, we will only discuss here the evolution of damage seen in the Si sublattice, i.e., centered around channel 450. As in Si, the damage level

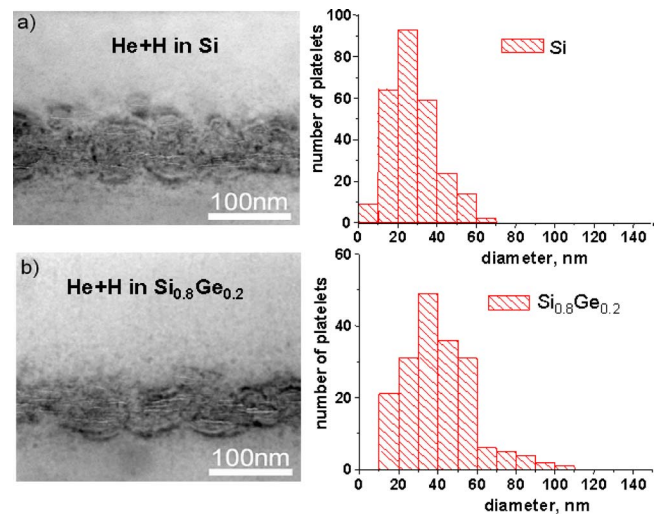


FIG. 5. (Color online) XTEM micrographs of annealed sequentially implanted samples.

in the as-implanted layers is much smaller after sequential implantation than after H-only implantation. Both damage levels increase during annealing but the increase in the amount of lattice disorder is considerably more significant for the sequential implant as compared to H-only implant. Again, the damage seen by RBS after annealing is somewhat sharper in the sample sequentially implanted.

It has been previously shown that, for H-only implants in Si and SiGe, the H profiles do not change significantly during annealing at moderate temperature.^{9,11} Figure 4 shows the SIMS profiles of H and He obtained after sequential implantations in Si [Fig. 4(a)] and SiGe [Fig. 4(b)] samples in the as-implanted state and after annealing at moderate temperature. There is little difference between H depth profiles in the as-implanted and annealed (not shown in Fig. 4) states. However, we note a large redistribution of implanted He during annealing: migration toward and accumulation in the region corresponding to the maximum in H concentration. This phenomenon is better evidenced in the SiGe sample, where the distance between the maxima of the H and He profiles is twice larger than in Si.

Figure 5 shows a set of typical XTEM images of the He+H sequentially implanted Si and SiGe samples after the same annealing [Figs. 5(a) and 5(b)] and the size histograms describing the populations of platelets in these samples. After annealing at moderate temperature, the mean size of the platelets is significantly larger in SiGe (40 nm) than in Si (27 nm). Conversely, the area density of platelets is smaller in SiGe than in Si: 5.5×10^{10} and $11 \times 10^{10} \text{ cm}^{-2}$, respectively. Moreover, the width of the zone in which the platelets are confined is smaller in SiGe than in Si (60 and 80 nm, respectively). We conclude from these observations that the Ostwald ripening of platelets created by the sequential implantation of He and H is faster in SiGe than in Si.

IV. DISCUSSION

The data on splitting kinetics presented in Fig. 1 clearly show that the process of layer transfer depends strongly on the properties of the corresponding materials and the nature

of the implanted species, i.e., H-implant or sequential implant He+H. XTEM images [Figs. 2(a) and 2(b)] do not show significant differences between the populations of platelets observed in H-only implanted samples, Si and SiGe, after annealing at moderate temperature. The difference in splitting kinetics cannot be directly ascribed to differences in H diffusivity or platelet growth rate as the diffusivities of all relevant species involved in that growth (H and vacancies) are larger in SiGe than in Si. We note, however, that the depth distribution of platelets is wider in SiGe than in Si, an observation consistent with the larger surface roughness of the SiGe samples after splitting.⁹ The reason for slower splitting in SiGe is not due to the behavior of H-related defects but to the reaction of the material itself to the stress exerted by a given population of defects. Indeed, stress relaxation by straining of the matrix is expected to be easier in SiGe than in Si owing to the weaker Si–Ge bond. An important observation concerns the presence of nanovoids and the platelet-like aligned nanovoids [Figs. 2(d) and 2(f)] in as-split SiGe when the annealing increases up to 500 °C. These platelet-like aligned nanovoids might be due to the breaking up of (001) platelets into small pores. That phenomenon was not detected in Si [Fig. 2(e)]. It is known that the propagation of fracture lines is due to formation of (001) hydrogen-terminated internal surface and pumping of gas (H₂) in it.¹¹ We speculate that, at the later stages of the layer transfer, due to the lower thermal stability of the Si–H bond the hydrogen-terminated (100) internal surface in Si_{0.8}Ge_{0.2} changes its morphology. Si in the matrix tends to close up other nearby Si, resulting in a decrease in the size and density of these platelets. In contrast, for Si, the Si–H bond of (100) hydrogen-terminated internal surface is more stable even at 650 °C.¹² The loss of many platelets favorable for exfoliation at this moment provides an explanation of the slower splitting kinetics in SiGe with the H-only implant.

Thermal annealing of hydrogen implanted Si results in significant increase in the channelled-RBS signal. Cerofolini *et al.*¹³ attributed the origin of this effect to the formation of hydrogen molecules in vacancy agglomeration sites. Our RBS/channeling results in Fig. 3 indicate that significantly stronger reverse annealing effect is observed for the sequentially implanted samples, Si, and Si_{0.8}Ge_{0.2}, as compared to H-only ones. Despite a very low level of damage in the as-implanted state for sequential implants, the height of the damage peaks is comparable for both implant types after the short anneal at moderate temperature. The finding is very consistent with the TEM observation that the populations of platelets are much more confined in depth after sequential implantation (about 60–80 nm in Fig. 5) than after H-only implantation (about 210 nm in Fig. 2). Moreover, TEM also reveals that the platelets found after sequential implantation are much larger than those found after H-only implantation after the same annealing conditions. These two characteristics, larger platelets and better in-plane confinement of these platelets, explain well why splitting occurs faster after sequential implantation than after H-only implantation. It is well known that implantation with any kind of ion leads to formation of high strain closer to the implanted range. During sequential implantation, H is introduced in the region,

which is already strained by previous implantation of He. So, this region could be “doubly” strained. Of course, this works only in the case of sequential implantation and cannot be applied for H-only implantation. Alternatively, SIMS results show that the total redistribution of He during annealing occurs with characteristics consistent with the diffusion and trapping of the He atoms in a sharp region close to the H profile (Fig. 4). The “double strain” effect and massive transfer of He toward the H-rich region allow a faster growth of the H and He related platelets. Recent and in-depth characterization of quite similar samples by positron Doppler broadening spectroscopy (DBS) suggests that hydrogen atoms interact with the damage previously created by He implantation, producing more stabilized vacancylike defects, a finding consistent with our own observations.¹⁴

Diffusivity arguments only cannot be brought to the forefront to explain the different behaviors in splitting kinetics between Si and SiGe after sequential implantation since we ruled them out to compare splitting characteristics between H-only and sequential implantations in two materials. The migration length of He is larger in SiGe than in Si as measured by our SIMS results. However, for both in Si and SiGe, the phenomenon is not limited by He diffusion only as all the He atoms should be transferred during annealing from the implanted region toward the H-rich region. Interestingly, TEM shows that after the same implantation and annealing conditions, the platelets are significantly larger, in smaller density, and confined within a thinner layer in SiGe than in Si (Fig. 5). In other words, the Ostwald ripening of the platelets, known to be at the origin of the formation of microcracks and further splitting, goes faster in SiGe than in Si after sequential implantation, while this could not be evidenced after H-only implantation.

The nucleation and/or the Ostwald ripening of the He–H platelets are/is limited by the availability and diffusivity of one of the species involved in that competitive growth. Platelet nucleation and growth occur through the coprecipitation of gas atoms (H and/or He) and vacancies.^{11,15} Our TEM and SIMS results show that the behavior of H is quite similar in H-only implanted Si and SiGe samples after annealing at moderate temperature, although some small differences in binding energies exist. We do not expect that He behaves radically differently in SiGe than in Si. Thus, we are left with the possibility that vacancies may play the central role in controlling the kinetics of platelet growth and splitting. The formation of vacancies and vacancy clusters has been studied in detail in SiGe.¹⁶ It is known that the most abundant defect is a monovacancy surrounded by four Ge atoms, whose formation energy is 1 eV lower than that of V–Si₄ due to the weakening of the atomic bonding. Consequently at any given temperature the equilibrium concentration of vacancies is higher in SiGe alloys than in pure Si layer, and this facilitates the nucleation and/or increases the growth rate of the gas-filled cavities during annealing and leads to faster splitting in SiGe.

That result does not contradict that for H-only implanted samples. In the sequentially implanted samples, the fracture line was already observed after annealing at moderate temperature (300–400 °C) due to the massive transfer of He

toward the H-rich region. So the layer transfer takes place at the temperature significantly lower than that corresponding to the dissolution of fracture defining (001) platelets in SiGe with H-only implantation, i.e., near 500–550 °C.

V. SUMMARY

The mechanism of the Si_{0.8}Ge_{0.2} layer transfer in the Smart Cut™ technology for H-only and sequential He+H implants was studied using a wide range of techniques. Taking into account recently published results, we propose a scenario that explains the observed behavior. For H-only implants, the slower splitting in SiGe than in Si is due to the reaction of the material itself to the stress exerted by a given population of defects in this material. Alternatively, after sequential He+H implantation, this effect is overcompensated by the faster growth kinetics of gas-filled platelets, a behavior we correlated with the “double strains” effect and fast diffusion and total getting of He into the H-rich and/or V-rich regions. In all cases, sequential implantation at low dose permits faster splitting kinetics in Si and SiGe than H-only implantation. Moreover, the larger concentration of vacancies available in the SiGe samples facilitates the nucleation and/or increases the growth rate of the gas-filled cavities during annealing, leading to faster splitting in SiGe sequentially implanted sample with regard to pure Si.

¹J. Welser, J. L. Hoyt, and J. F. Gibbons, *IEEE Electron Device Lett.* **15**, 100 (1994).

²W. Xiong, C. R. Cleavelin, P. Kohli, C. Huffman, T. Schulz, K. Schrufer, G. Gebara, K. Mathews, P. Patruno, I. Cayrefourcq, M. Kennard, C. Mazure, K. Shin, and T.-J. King Liu, *IEEE Electron Device Lett.* **27**, 612 (2006).

³A. V-Y. Thean, D. Zhang, V. Vartanian, V. Adams, J. Conner, M. Canonico, H. Desjardin, P. Grudowski, B. Gu, Z.-H. Shi, S. Murphy, G. Spencer, S. Filipiak, D. Goedeke, X.-D. Wang, B. Goolsby, V. Dhandapani,

L. Prabhu, S. Backer, L.-B. La, D. Burnett, T. White, B.-Y. Nguyen, B. E. White, S. Venkatesan, J. Mogab, I. Cayrefourcq, and C. Mazure, *VLSI Tech. Symp. Proc.*, 2006, p. 130.

⁴F. Andrieu, T. Ernst, O. Faynot, Y. Bogumilowicz, J.-M. Hartmann, J. Eymery, D. Lafond, Y.-M. Le Vaillant, C. Dupre, R. Powers, F. Fournel, C. Fenouillet-Beranger, A. Vandooren, B. Ghyselen, C. Mazure, N. Kernevez, G. Ghibaudo, and S. Deleonibus, *Proceedings of the IEEE International SOI Conference*, 2005, p. 223.

⁵B. Ghyselen, J.-M. Hartmann, T. Ernst, C. Aulnette, B. Osternaud, Y. Bogumilowicz, A. Abbadie, P. Besson, O. Rayssac, A. Tiberj, N. Daval, I. Cayrefourcq, F. Fournel, H. Moriceau, C. Di Nardo, F. Andrieu, V. Paillard, M. Cabié, L. Vincent, E. Snoeck, F. Cristiano, A. Rocher, A. Ponchet, A. Claverie, P. Boucaud, M.-N. Semeria, D. Bensahel, N. Kernevez, and C. Mazure, *Solid-State Electron.* **48**, 1285 (2004).

⁶L. J. Huang, J. O. Chu, D. F. Canaperi, C. P. D’Emic, R. M. Anderson, S. J. Koester, and H.-S. Philip Wong, *Appl. Phys. Lett.* **78**, 1267 (2001).

⁷G. Taraschi, A. J. Pitera, L. M. McGill, Z.-Y. Cheng, M. L. Lee, T. A. Langdon, and E. A. Fitzgerald, *Novel Materials and Processes for Advanced CMOS*, MRS Symposia Proceedings, Vol. 745 (Materials Research Society, Pittsburgh, 2003), p. N4.7.1.

⁸R. Singh, I. Radu, M. Reiche, R. Scholz, D. Webb, U. Gösele, and S. H. Christiansen, *Mater. Sci. Eng., B* **124–125**, 162 (2004).

⁹P. Nguyen, C. Aulnette, E. Guiot, N. Daval, K. K. Bourdelle, I. Cayrefourcq, C. Deguet, S. Sartori, A. Tauzin, C. Lagahe-Blanchard, and A. Soubie, *Silicon-on-Insulator Technology and Devices XII*, ECS Proceedings, Vol. 2005-03 (The Electrochemical Society, Pennington, NJ, 2005), p. 185.

¹⁰J. Grisolia, G. Ben Assayag, A. Claverie, B. Aspar, C. Lagahe, and L. Laanab, *Appl. Phys. Lett.* **76**, 852 (2000).

¹¹S. Personnic, K. K. Bourdelle, F. Letertre, A. Tauzin, N. Cherkashin, A. Claverie, R. Fortunier, and H. Klocker, *J. Appl. Phys.* **103**, 023508 (2008).

¹²M. K. Weldon, V. E. Marsico, Y. J. Chabal, A. Agarwal, D. J. Eaglesham, J. Sapjeta, W. L. Brown, D. C. Jacobson, Y. Caudano, S. B. Christman, and E. E. Chaban, *J. Vac. Sci. Technol. B* **15**, 1065 (1997).

¹³G. F. Cerofolini, L. Meda, R. Balboni, F. Corni, S. Frabboni, G. Ottaviani, R. Tononi, M. Anderle, and R. Canteri, *Phys. Rev. B* **46**, 2061 (1992).

¹⁴C. Macchi, S. Mariazzi, G. P. Karwasz, R. S. Brusa, P. Folegati, S. Frabboni, and G. Ottaviani, *Phys. Rev. B* **74**, 174120 (2006).

¹⁵C. Villeneuve, K. K. Bourdelle, V. Paillard, X. Hebras, and M. Kennard, *J. Appl. Phys.* **102**, 094905 (2007).

¹⁶M. Rummukainen, J. Slotte, K. Saarinen, H. H. Radamson, J. Hallstedt, and A. Yu. Kuznetsov, *Phys. Rev. B* **73**, 165209 (2006).